Monitoring of cellulose-rich biowaste co-digestion with 3D fluorescence spectroscopy and mass spectrometry-based metabolomics

Olivier Chapleur, Angéline Guenne, Douglas N Rutledge, Francesc Puig-Castellví

Monitoring of cellulose-rich biowaste co-digestion with 3D fluorescence spectroscopy and mass spectrometry-based metabolomics

Olivier Chapleur,[1] Angéline Guenne,[1] Douglas N. Rutledge,[2,3] Francesc Puig-Castellví [1,4,5,]*

[1]Université Paris-Saclay, INRAE, PRocédés biOtechnologiques au Service de l'Environnement, 92761 Antony, France

[2]Faculté de Pharmacie, Université Paris-Saclay, 91400 Orsay, France

[3]Muséum National d'Histoire Naturelle, 75005 Paris, France

[4]Université Paris-Saclay, INRAE AgroParisTech, UMR SayFood, 75005 Paris, France

[5]Present address: EGENODIA Inserm U1283, CNRS UMR8199, Institut Pasteur de Lille, Lille University Hospital, European Genomic Institute for Diabetes (EGID), Université de Lille, 59045, Lille, France

**Corresponding Author. Tel:+33 0320974242, email address: francesc.puig-castellvi@inserm.fr*

Abbreviations

3D EEM: Three dimensional excitation emission matrix

AD: Anaerobic digestion

AcoD: Anaerobic co-digestion

FW: Food waste

HPLC: High performance liquid chromatography

MS: Mass spectrometry

Abstract

Anaerobic digestion (AD) is a promising waste management strategy that reduces landfilling while generating biogas. Anaerobic co-digestion involves mixing two or more substrates to enhance the nutrient balance required for microorganism growth and thus improve the degradation. Monitoring AD is crucial for comprehending the biological process, optimizing process stability, and achieving efficient biogas production. In this work, we have used three dimensional excitation emission fluorescence spectroscopy and mass spectrometry metabolomics, two complementary techniques, to monitor the anaerobic co-digestion (AcoD) of cellulose, ash wood or oak wood with food waste. The two approaches were compared together and to the biogas production records. Results of this experiment demonstrated the complementarity of both analytical techniques with the measurement of the biogas production since 3D fluorescence spectroscopy and MS metabolomics revealed the earlier molecular changes occurring in the bioreactors, mainly associated with the hydrolysis step, whereas the biogas production data reflected the biological activity in the last step of the digestion. Moreover, in all cases, the three data sets effectively delineated the differences among the substrates. While the two wood substrates were poorly degradable as they were richer in aromatic compounds, cellulose was highly degradable and was characterized by the production of several glycolipids. Then, the three tested AcoDs resulted in a similar 3D EEM fluorescence and metabolomics profiles, close to the one observed for the AD of food waste alone, indicating that the incorporation of the food waste drove the molecular degradation events in the AcoDs. Substrate-specific differences were appreciated from the biogas production data. The overall results of this research are expected to provide insight into the design of guidelines for monitoring AcoD.

Keywords

anaerobic digestion, food waste, wood, 3D EEM, metabolomics

Graphical abstract

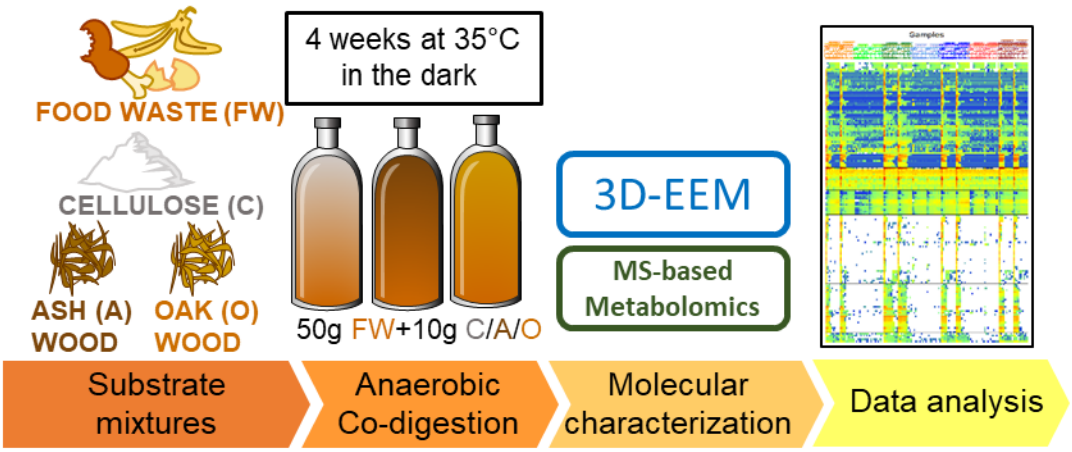

1. Introduction

The production of municipal solid waste grows around the world (Braguglia et al., 2018) . In 2017, biowaste in the 28 European Union member states accounted for more than 34 % of the municipal solid waste generated, or 86 million tonnes (EEA, 2020). Biowaste includes garden and park waste, food products and kitchen waste from households, restaurants and supermarkets, and comparable waste from food processing plants (EEA, 2020). Recycling biowaste is essential to achieve the EU's goal of recycling 65% of municipal waste by 2035 (EEA, 2020). Composting and anaerobic digestion (AD) are currently the two most widely applied techniques to reduce the amount of biowaste and minimize its landfilling (EEA, 2020). While composting is more extended than AD, the use of the latter is increasing because it is a source of renewable energy as it produces biogas and because AD tends to deliver higher environmental benefits (Slorach et al., 2019).

Biowaste contains, depending on its origin, a mixture of readily biodegradable organic constituents (e.g., simple sugars, starch, proteins and lipids), more recalcitrant biopolymers (e.g., lignocellulose) and undesirable content (e.g., plastic, packaging) (Moretti et al., 2020). During anaerobic digestion, complex organic molecules are broken down into simpler compounds that are ultimately converted to methane and CO_2 by the microbial community living in the anaerobic digesters (Chatterjee and

Mazumder, 2019). Biogas production in anaerobic digesters depends on the capacity of the microbial community to degrade the waste. To increase the degradability of the more recalcitrant waste, it can be digested in combination with more biodegradable substrates. This strategy is known as anaerobic co-digestion (AcoD) and is considered to be very environmentally efficient as it allows for the simultaneous processing of multiple types of waste (Borowski and Kubacki, 2015).

A current challenge in AcoD is its optimization for a maximal methane yield while also maintaining process stability and better handling of wastes. In this aim, it is important to monitor anaerobic digesters during AcoD for understanding their functional behavior, that has a direct impact for efficient biogas production (Cruz et al., 2021). So far, AD is mainly assessed by the inspection of several parameters such as pH, alkalinity, volatile fatty acid concentrations, biogas composition, and the composition of the microbial community (Awhangbo et al., 2020). While these parameters can provide information about the digester stability, they are not descriptive of the specific molecular events occurring during the waste degradation and, thus, they cannot fully explain the underlying cause that resulted on the measured reactor's disturbance (i.e., pH acidification, low methane yield production). To do so, several analytical techniques have been proposed to characterize the molecular composition of biological samples. For example, spectroscopic techniques can be used to pinpoint the functional groups in the compounds present in the studied samples (e.g., infrared, ultraviolet and fluorescence spectroscopies) (Madsen et al., 2011). Mass spectrometry can also be employed to identify the small compounds in the samples (Du et al., 2023).

Three dimensional excitation emission fluorescence spectroscopy and mass spectrometry are two techniques whose combined use for the study of AD is promising. 3D fluorescence spectroscopy generates 3D excitation-emission matrices (3D EEM) which can provide information about the structural complexity of the organic matter, characterizing its degradation capabilities (Maynaud et al., 2017). Then, mass spectrometry provides a comprehensive view of the specific compositional changes occurring during biowaste degradation. 3D EEM fluorescence spectroscopy can be used to characterize the signature of macromolecules such as fulvic acid and proteins (Muller et al., 2014), while mass spectrometry reveals the changes in the smaller molecules (Puig-Castellví et al., 2020).

This application of mass spectrometry to characterize the small molecules in biological samples is known as mass spectrometry metabolomics (Dettmer et al., 2007).

The potential of these techniques for the waste management field has resulted in a few recent publications on their use in anaerobic digestion. In Li et al. (2023) and Zhao et al. (2023), the anaerobic digestion of wastewater sludge was studied with 3D EEM spectroscopy and Fourier transform ion cyclotron resonance mass spectrometry. Having said this, wastewater sludge and biowaste are two very different substrates. In addition to biomass (e.g. fibers, proteins, fats) found in both substrates (Bhatia et al., 2018; Rorat et al., 2019), wastewater sludge can contain considerable amounts of emerging contaminants such as phthalates, organic nanoparticles and surfactants, among other chemicals (Rodriguez-Narvaez et al., 2017). Due to the presence of these compounds in wastewater sludge and to a lower protein content than in biowaste, the latter is generally more efficiently degraded than the former (Iacovidou et al., 2012). In this context, the use of these two analytical techniques could result in a better understanding of each specific AcoD process (e.g., to examine the inhibitory effects of heavy metals and other compounds, and to characterize the degradation profile of contaminants in the sludge). This knowledge could then lead proposals for new process strategies to improve overall process efficiency (e.g., changing the substrate/co-substrate ratio (Puig-Castellví et al., 2020) or other operational parameters such as the reactor's temperature (Puig-Castellví et al., 2022), or using bio-augmentation or additional substrate pretreatments to facilitate the degradation of a specific family of compounds). To our knowledge, these two techniques have never been used simultaneously to study the AD of biowaste.

In order to obtain insight about the molecular processes in the context of the AcoD of biowaste and their implications in biogas production, we have explored the digestion of three cellulosic substrates (cellulose, and sawdust from ash (*Fraxinus spp.*) and oak (*Quercus spp.*) trees employing food waste (FW) as their co-substrate with 3D fluorescence spectroscopy and mass spectrometry metabolomics. Therefore, the main objectives of this study were to (1) evaluate the performance of the investigated AcoD conditions, (2) analyze the temporal changes in the molecular composition of the substrates and assess the complementarity of the two techniques, and (3) relate the observed changes to the variations

in biogas production. The results from this study would provide significant guides for studying biowaste degradation from a molecular perspective, with potential applications for the development of a monitoring tool aiming to improve process efficiency in waste management.

2. Material and methods

2.1. Feedstock preparation and experimental set-up

FW was provided by an industrial food waste collector (Valdis Energie, Issé). Cellulose was alpha cellulose (Sigma-Aldrich). Ash and oak wood was shredded sawdust collected at a local sawmill processing these two types of wood. The inoculum used in the study was obtained from a mesophilic 60 L laboratory anaerobic bioreactor fed with similar FW. For the experimental set-up, a total of 14 anaerobic batch bioreactors, each consisting of 1 L glass bottles, were used. In this study, 7 different substrate compositions are tested in duplicate: the four mentioned substrates, and three binary mixtures containing FW with either cellulose, ash wood or oak wood. Bioreactors dedicated to mono-digestions contained 52.2 g of FW, 10 g of cellulose, 10 g of ash wood or 10 g of oak wood, corresponding respectively to 12, 4.6, 5.8 or 6.3 grams of Chemical Oxygen Demand (gCOD) (LCK514 DCO test kit, Hach Lange). Binary mixtures used in the remaining bioreactors were prepared by blending together a quantity of each substrate similar to the one used for mono-digestion. Then, all 14 bioreactors were inoculated with 60 g (1.2 gCOD) of anaerobic sludge. All the bioreactors were complemented with a biochemical potential buffer (International Standard ISO 11734 (1995) (International Organization for Standardization, Geneva, 1995)) up to a final volume of 700 mL. Bioreactors were sealed with a screw cap and a rubber septum and headspaces were flushed with N_2 (purity > 99.99%, Linde gas SA), and incubated for 4 weeks at 35°C in the dark without agitation. Daily biogas productions were measured with a Gas Endeavour® (BCP Instrument).

2.2. Sampling

Sampling was carried out at days 0, 3, 7, 10, 14, 17, 21, 24, 28 and 31. Sampling was performed by collecting 10 mL of liquid phase from the digester through the septum using a syringe. Then samples were centrifuged at 10,000 g for 10 min at 4°C to collect the supernatants, which were then snap frozen in liquid nitrogen and kept at -20ºC prior the 3D EEM fluorescence and metabolomic analyses. The 14 bioreactors and the 10 sampling dates resulted in a total of 140 samples being collected.

2.3. 3D fluorescence analysis

3D fluorescence spectra were measured directly on the thawed samples without prior chemical treatment, using a Xenius spectrofluorometer (SAFAS, Monaco) equipped with a xenon lamp source, excitation and emission monochromators and a front face sample-cell holder. Measurements were carried out in triplicate using a quartz cuvette. The instrumental settings were: excitation range 240–600 nm, emission range 210–620 nm, wavelength increments 3 nm, spectral slits 3 nm, automatic (EX) and open (EM) filter positions, and PMT voltage 420 V.

2.4. MS metabolomic analysis

One mL of each sample was diluted with 4 mL of double-distilled H_2O. The resulting samples were then filtered with 0.45 μM Nylon filters and stored at -80°C until the HPLC-MS analyses were conducted. HPLC-MS samples were prepared by mixing 500 μl of each sample with an equal amount of acetonitrile (ACN). Quality Control samples (QCs), formed by pooling all individual samples, were also prepared. The instrumental setup consisted of an Accela 1250 pump system connected to an LTQ-Orbitrap XL mass spectrometer (Thermo Scientific, Waltham, MA, USA) operated in positive electrospray ionization mode (ESI+). Detection was performed in full scan over an m/z range from 50 to 800 at a resolution of 60,000. A NUCLEODUR HILIC column (100 mm x 2.1 mm ID, particle size 1.8 μm) provided with a NUCLEODUR HILIC guard column (4 mm x 2.1 mm ID, particle size 1.8 μm) (Macherey-Nagel, Düren, Germany) was used. Mobile phases used were milli-Q ACN (phase A) and water containing 50 mM ammonium acetate at pH 5.0 (phase B). For each sample, 10 μL were

injected. The flow rate was set at 0.4 mL min-1. The HPLC gradient started at 5 % B and held for 3 min, then increased to 40 % B during 11 min. From minutes 14 to 24, B was linearly decreased to 5 %. Finally, initial conditions were re-equilibrated in 5 minutes, resulting in a total run time of 29 min. To remove possible batch effects, samples were injected in random order. Moreover, Quality Controls (QCs) and blanks were injected every 8 samples. In total, 181 samples were injected (140 samples, 19 QCs and 22 blanks).

Raw HPLC-MS data were converted into mzXML-format files using MSConvert (ProteoWizard 3.0). Then, chromatographic features were extracted using the XCMS Online platform.

2.5. Data pretreatment and analysis

2.5.1. Fluorescence dataset

Each 3D fluorescence spectrum can be regarded as a matrix, where the columns and rows describe the excitation (121 wavelengths) and corresponding emission (125 wavelengths) spectra, respectively. For every fluorescence spectrum, Rayleigh and Raman scatterings were removed and replaced by interpolation of the surrounding data using a three-dimensional Delaunay triangulation method, as described in Zepp et al., 2004. Each set of triplicate technical spectra were averaged and unfolded into a vector, and the vectors for the 140 samples (14 bioreactors times 10 time-points) were concatenated column-wise keeping in common the same emission and excitation wavelengths. Spectral points containing intensity values lower than 40 for all the samples were removed. After this variable removal, the dataset had 140 rows and 7331 columns. Next, this dataset was SNV-transformed and analyzed by Independent Components Analysis (ICA) (Rutledge and Jouan-Rimbaud Bouveresse, 2013).

ICA is a blind source chemometric method used for separating mixed signals into their underlying source signals and the proportions (or scores). In this context, the JADE algorithm, one of the several methods available for calculating ICA models, was employed. (Rutledge and Jouan-Rimbaud Bouveresse, 2013). The determination of the optimal number of Independent Components (ICs) to use

is a key step for building an ICA model. This number was determined using both the Durbin–Watson criterion (Jouan-Rimbaud Bouveresse et al., 2012) and the random ICA method (Kassouf et al., 2018). In order to explore the ICA results at the variable level, the ICA signals were refolded (filling the empty spaces due to the variable removal with 0s) so as to recover the matrix structure of the original 3D fluorescence spectra.

2.5.2. LC-MS metabolomics dataset

The metabolomics dataset, with 140 samples in rows and 1947 LC-MS features in columns, was examined using two complementary strategies.

A first strategy was applied to identify the main metabolite degradation trends occurring in the bioreactors. In this strategy, the matrix was auto-scaled and analyzed by Principal Components Analysis (PCA) (Peris-Díaz and Krężel, 2021). Then, for each principal component (PC), chromatographic features with loading values beyond 2 standard deviations were considered to be representative of these degradation trends (Puig-Castellví et al., 2020).

A second strategy was used to determine the features that enable the discrimination of the two wood types. In this case, a subset of the metabolomics dataset was created by selecting those samples containing either oak or ash wood (in presence or not of FW) that had been collected on the first sampling day. This dataset was auto-scaled and subsequently analyzed with Orthogonal Partial Least Squares-Discriminant Analysis (O-PLS-DA). This analysis was performed using the opls function from the *ropls* package in R (Thévenot et al., 2015). LC-MS features with Variable Importance in Projection (VIP) values above 2 were considered to be drivers of the sample discrimination and their temporal profile over the 31 days was inspected in a heatmap.

For both strategies, features were tentatively annotated using the LC-MS search tool from HMDB (Wishart et al., 2022).

3. Results

3.1. Biogas production

The daily biogas production profile in **Figure 1** reflects the efficiency and performance of the anaerobic digestion process. Early peaks in this profile correspond to highly degradable compounds, while later peaks are associated with less accessible ones. Profiles without significant peaks indicate a highly recalcitrant composition.

The biogas production varied over time and could be categorized into four temporal periods: early degradation (days 1 to 4), the immediate period following early degradation (approximately days 4 to 10), mid-degradation (approximately weeks 2 to 3), and late degradation (after 3 weeks).

During the early degradation stage, biogas production exhibited a prominent peak in FW-containing digestions, approximately 15-25 times larger than in equivalent mono-substrate digestions. In the second degradation period, cellulose had the highest biogas production peak (600 mL/day at day 7), followed by FW-cellulose (approximately 230 mL/day at day 5). Oak and ash mono-digestions also had peaks in this period (14 mL/day at day 7 for oak AD and 36 mL/day at day 10 for ash AD).

The mid-degradation phase was primarily observed in reactors containing FW, showing a wide, continuous peak throughout this period. FW AD reached a peak of 626 mL/day on day 13, while the corresponding peaks for FW co-digestions appeared slightly later (day 15 for FW-ash AD and day 17 for FW-oak and FW-cellulose ADs). Ash AD also had a peak, but it was approximately 10 times smaller than that of FW-containing digestions.

In the final degradation period, production peaks were observed in cellulose-containing digesters, similar to the second degradation period. However, the maximum biogas production was higher in co-digestion systems (the contrary of the observed in the second degradation period), reaching around 1000 mL/day, while the corresponding mono-digestions achieved levels of approximately 300 mL/day.

Considering the total amount of biogas produced in the AcoD systems compared to the sum of the mono-digestion counterparts, FW-oak resulted in slightly higher biogas production (8407 mL for AcoD versus 8163 mL for the sum of the FW and oak mono-digestions). In contrast, FW-ash and FW-cellulose produced less biogas compared to when each substrate was degraded separately, averaging 7900 mL versus 8525 mL and 11034 mL versus 12459 mL, respectively, for the FW-ash and FW-cellulose comparisons.

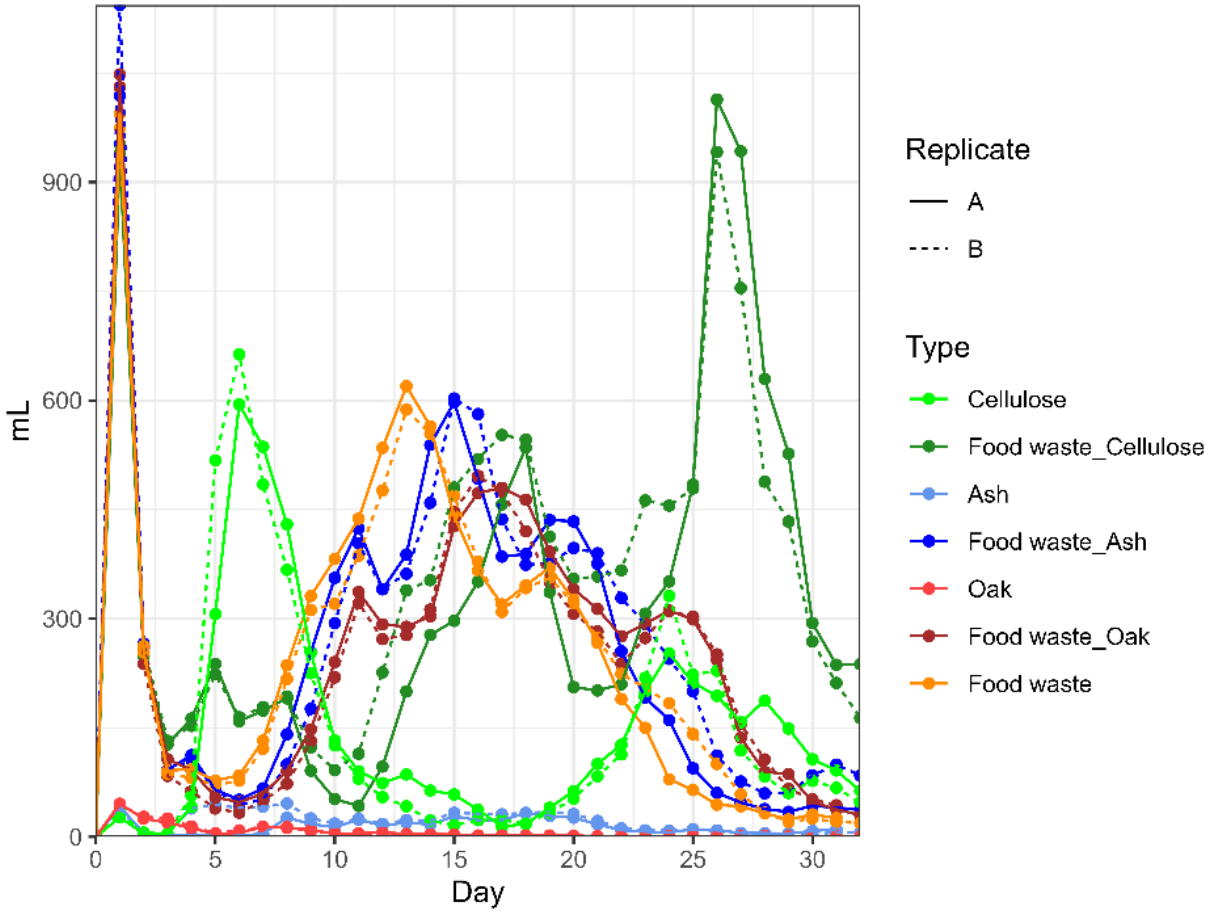

Figure 1. Daily biogas production.

3.2. 3D fluorescence spectroscopy

The fluorescence data provides information about the degradation of fluorescent compounds in the bioreactors, such as proteins and other more recalcitrant substances like humic acids (Muller et al., 2014). These data were analyzed by ICA to extract the degradation profiles of these compounds

(**Figure 2** and **3**), using 6 ICs for building the ICA model. Each independent component (IC) is composed of a vector of IC proportions, or scores (**Figure 2**), describing the temporal evolution of a compound, and a vector of IC signals (**Figure 3**), which contains the 3D EEM signature of that compound.

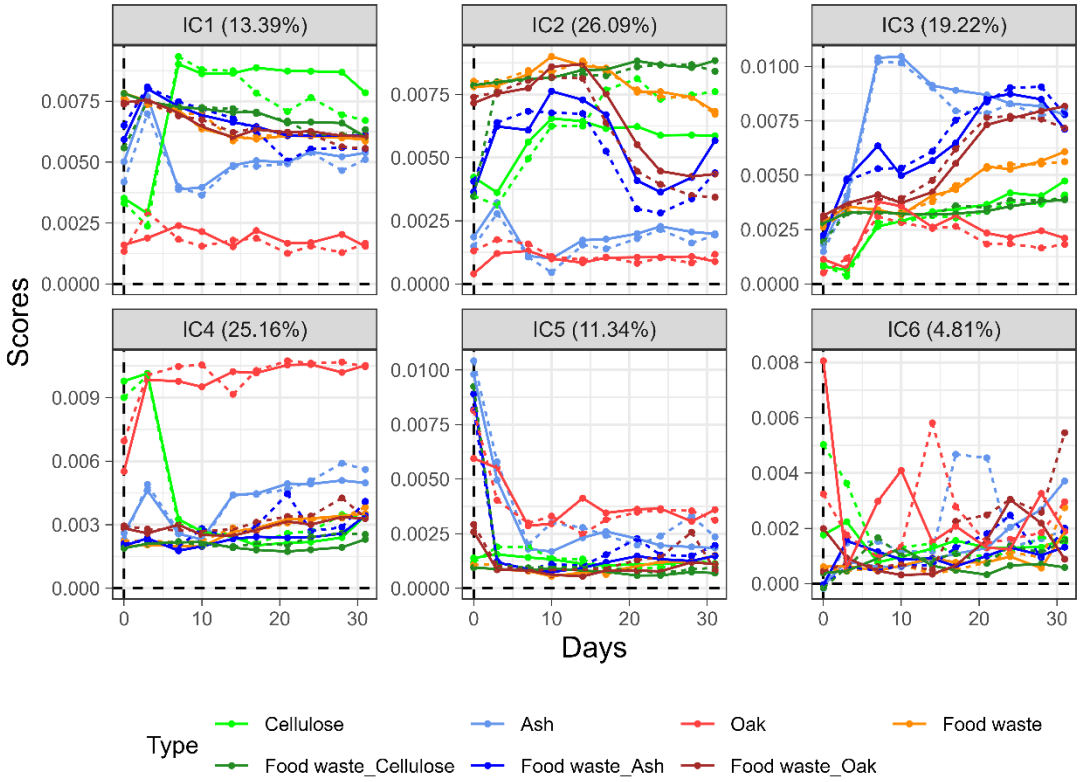

Figure 2. Temporal evolution of the ICA scores of the 3D fluorescence data. Replicates are depicted with different line types.

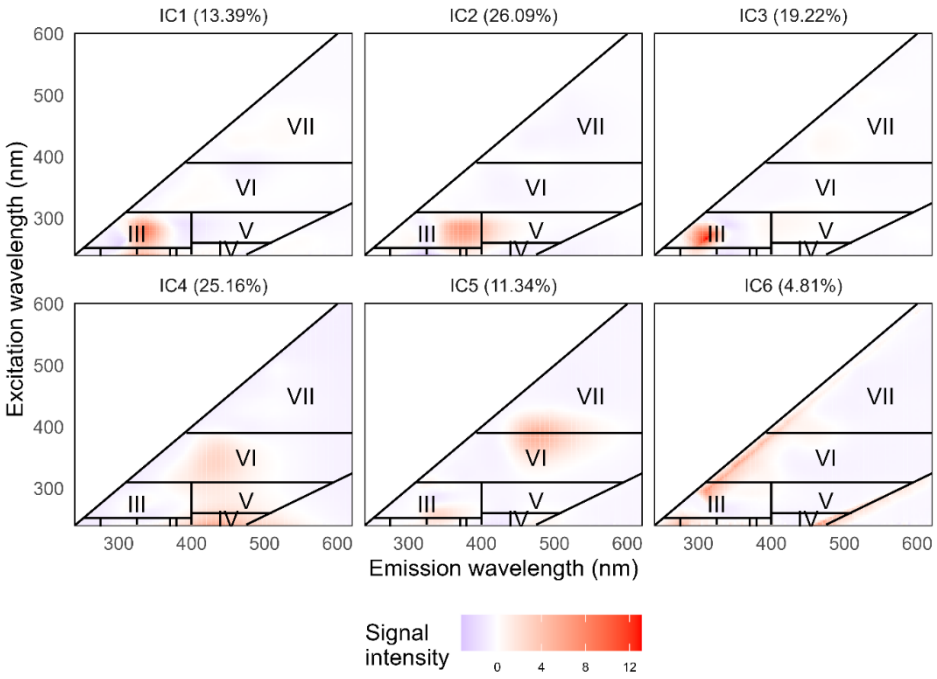

Figure 3. ICA signals of the 3D fluorescence data. Regions I-III: protein-like content; regions IV-V: fulvic-acid-like content; region VI: glycated protein-like molecules, lignocellulose-like and humic acid-like compounds; region VII: humic-like and lipofuscin-like materials.

Each of the components can be linked to one or a few molecular groups of compounds depending on the spectral fingerprint associated with them (Muller et al., 2014). Components IC1 (13.39% of the explained variance), IC2 (26.09%) and IC3 (19.22%) are characteristic of signals from region III, attributed to the protein-like content in the samples. The maxima of these signals are at wavelengths of λ_{EX}=282nm and λ_{EM}=334nm for IC1, λ_{EX}=279nm and λ_{EM}=373nm for IC2, and λ_{EX}=267nm and λ_{EM}=311nm for IC3, respectively (top panels in Figure 3). IC4 (25.16% of the explained variance) is descriptive of two signals, one from region IV (λ_{EX}=240nm and λ_{EM}=439nm) and another from region VI (λ_{EX}=345nm and λ_{EM}=436nm) (bottom left panel in Figure 3). The signal from region IV is attributed to fulvic-acid-like material while that from region VI can represent glycated protein-like molecules, lignocellulose-like and humic acid-like compounds. IC5 (11.34%) is defined by a peak comprised between regions VI and VII (λ_{EX}=387nm and λ_{EM}=475nm) (bottom middle panel in Figure 3). Region VII represents humic-like and lipofuscin-like materials (e.g., oxidized proteins and lipids). Lastly, IC6 (4.81%) captured the residual signals of the Rayleigh and Raman scatterings (bottom right

275 panel in Figure 3). The residual nature of IC6, rather than chemical, can also be appreciated from the
276 erratic behavior of the scores over time (bottom right panel in Figure 2), as opposed to the more
277 structured score profiles in the other 5 ICs.

278 The temporal evolution of the ADs can be studied by examining the scores (Figure 2):

279 Regarding IC1, cellulose AD followed a sudden increase after the 4^{th} day and it remained the AD with
280 the largest scores for IC1. Then, the IC1 scores related to all FW-containing AD followed the same
281 trend, consisting of a constant slow decline over time. For ash AD, the temporal profile showed a first
282 maxima at the 4^{th} day, followed by a strong decrease, and a continued increase after that. Oak is the
283 substrate with the lowest IC1 scores, which remained stable during all the experiment.

284 Ash, oak and cellulose ADs followed a similar evolution in IC2, albeit at a lower magnitude,
285 compared to their corresponding IC1 scores. Then, the largest IC2 scores were found for FW, FW-oak
286 and FW-cellulose ADs. In all these ADs, they increased monotonically. This rise was maintained for
287 all the experiment for FW-cellulose while they started to decline at the 14^{th} day for the other two ADs,
288 more abruptly in FW-oak than in FW. The FW-ash AD followed a waving profile, starting at low
289 scores and with change of progression trends in day 14 and once again in day 21.

290 IC3 scores exhibited a steady pattern for the first 10 days of the experiments and started to increase
291 after that for most FW-containing ADs (except for FW-ash AD). From the slightest to the most
292 marked increase, the sequence of escalation was as follows: FW-cellulose, FW and FW-oak. A second
293 trend was followed by cellulose and oak ADs. These two ADs started at very low IC3 scores,
294 increasing after day 4 to reach the levels for FW AD. After day 7, oak AD decreased while cellulose
295 AD mimicked the profile of FW-cellulose AD. Ash AD manifested a strong increase during the first
296 week and was followed by a slower decline that reached the levels observed for FW-oak ADs in this
297 component. FW-ash temporal evolution shows a profile that includes trends already observed in the
298 corresponding ash and FW mono-digestions, with a first increase during the first days of the
299 experiment (as in ash AD), and another increase after day 10 (as in FW AD).

At the beginning of the experiment, IC4 has important contributions from cellulose and oak ADs (although more in the former), with very low contributions for the rest. After the day 4, IC4 scores rapidly decreased for cellulose AD, reaching the levels observed for the FW AcoDs, and rapidly increased for oak AD. The trend observed for cellulose AD was opposed to that seen in IC1 for the same substrate. After that, IC4 remained steady in all conditions except ash AD until the end of the experiment. In ash AD, the temporal profile resembled that of the same substrate observed in IC1 and IC2, with a small peak at day 4 and a continued increase after day 10. At the end of the experiment, IC4 scores for ash AD were about half of those obtained for oak AD.

IC5 temporal evolution is mostly specific to ash- and oak-containing ADs, although more important in the former. In all these digesters, IC5 scores decreased rapidly at the beginning and remained stable for the rest of the experiment.

3.3. LC-MS metabolomics

Metabolomics, similarly to 3D fluorescence spectroscopy, can provide information about the degradation processes in waste materials. Rather than identifying the general groups of molecules being modified during the degradation, metabolomics highlights the specific molecules involved in the degradation process, to the extent that is possible to pinpoint the main degradation processes as well as determining how they are for each of the tested substrates.

As in the case of the 3D fluorescence data, the metabolomics data was first explored using PCA. The first two components of the PCA on the metabolomics data (**Figure 4**) explained 18.6% of the total dataset variance, meaning that the metabolomics data is the result of more biological processes than the 3D fluorescence data. In the PCA scores plot, PC1 separates samples containing FW (positive PC1 scores) from those that do not (negative PC1 scores). PC1 scores from cellulose, ash and oak samples collected at the beginning of the digestion are clustered together. The PC1 scores of the oak and ash samples did not substantially change over time, while the PC1 scores of the cellulose digestion samples evolved towards more negative values. On the other hand, PC2 mainly describes the temporal

evolution of samples containing FW, which go from negative to positive scores over time. Among them, the addition of oak or cellulose to FW did not produce an evident change in the metabolomics profile of the digestion. However, in the case of FW-ash AcoD, this caused a more dilated evolution in the PC2 dimension. At later time-points, the PC2 values became significantly more positive compared to the other digestion setups containing FW. PC2 does not reveal any consistent metabolic changes in the cellulose, ash and oak woods bioreactors.

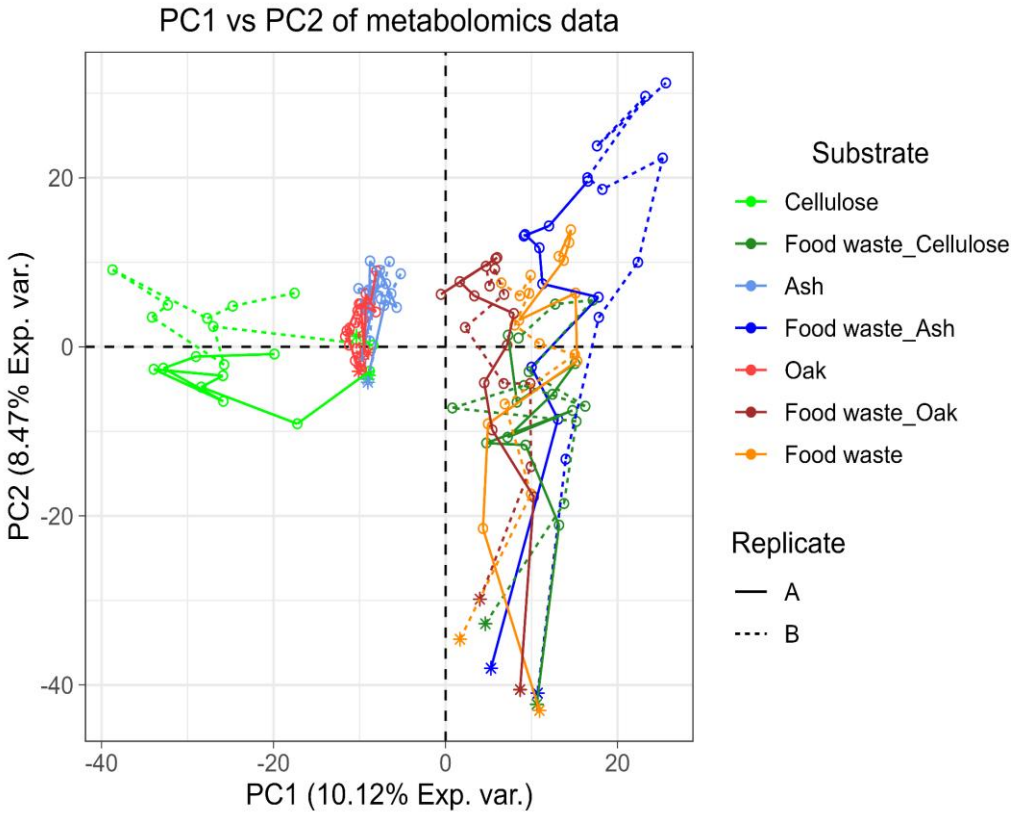

Figure 4. PCA scores of the metabolomics data. Samples from the first day are denoted with stars (instead of circles). Chronologically consecutive samples are connected with lines.

In order to further investigate the metabolic changes observed, the most representative LCMS features from PC1 and PC2 were plotted using heatmaps (**Figure 5**). 113 LCMS features were selected from PC1 and 145 features from PC2, based on their VIP.

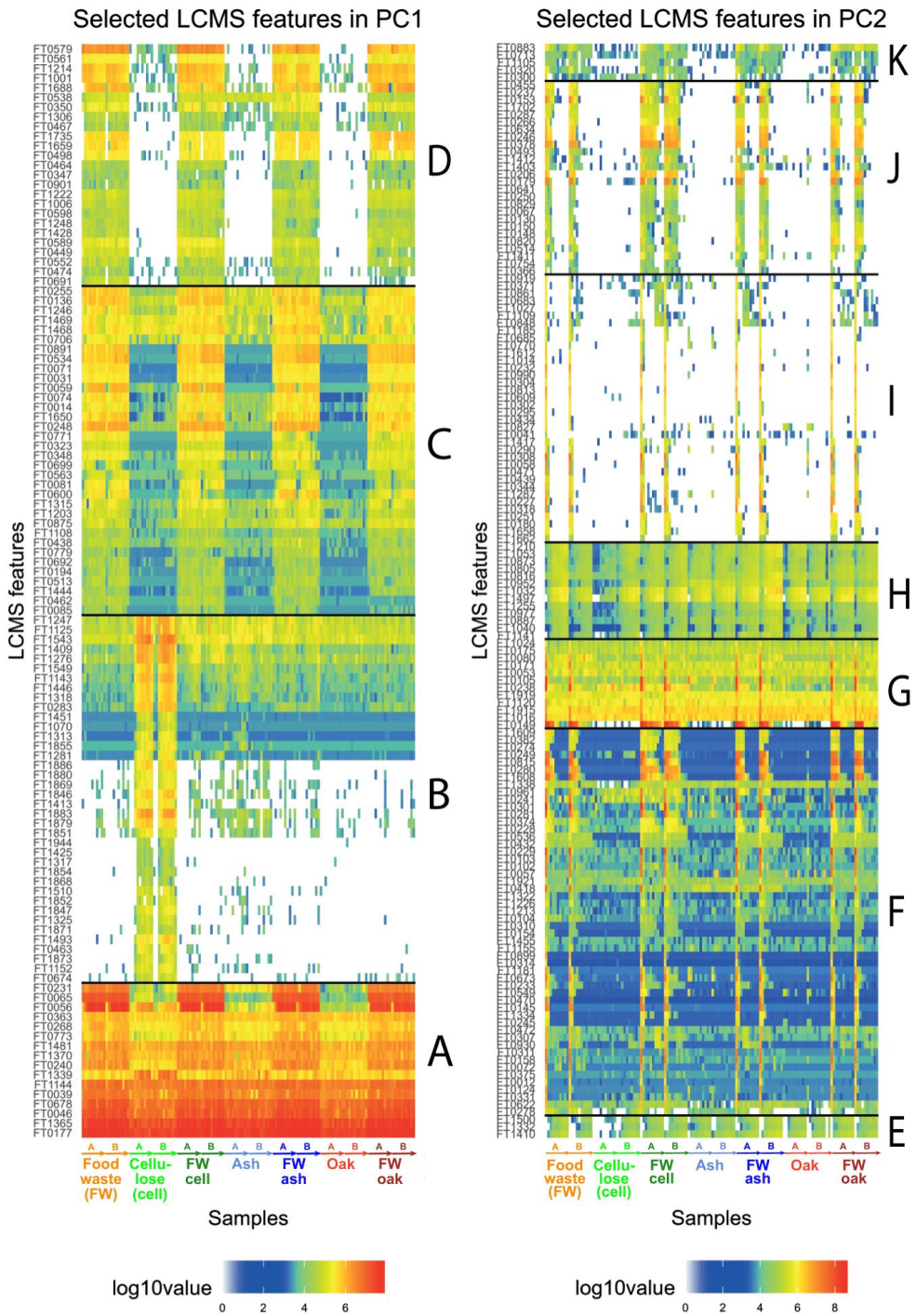

Figure 5. Heatmaps of the selected features in PC1 and PC2. Samples from each reactor are grouped and sorted by time. A and B stand for the replicates.

LCMS PC1 features can be classified into four different groups (A-D, **Figure 5A**). Metabolites in group B are more abundant in cellulose-only containing samples, while metabolites in groups A, C and D are more abundant in the FW-containing reactors. From a structural level, metabolic diversity

varies across the three groups. Among other compounds, group B contains glycosylated compounds (e.g., ceramides), group A has several adducts of phosphoric acid and short alkenes, group C has oxidized fatty acids, and group D contains quinolines, polycyclic structures (napthyls, phenantrenes) and some glycerolypids). More detail about the annotated metabolites can be consulted in **Table A.1**. Similarly, PC2 features can be classified into 7 groups (E-K, **Figure 5B**), depending on whether they are being accumulated or consumed over time, their presence at the first sampling date, how long their accumulation or consumption lasted, and on whether they were specific to biowaste–containing bioreactors. A summary of the main differences across groups is given in **Table1**. More detail about the annotated metabolites in PC2 can be consulted in **Table A.1**.

Table1. Groups of metabolites according to their evolution in PC2.

Group	Temporal evolution	Detection at day 0	Progression stopped after	FW-specific	Metabolite examples
E	Accumulation	No	3 days	No	oxidized C20-fatty acids
F	Consumption	Yes	3-14 days	No	taurine, lysine
G	Consumption	Yes	3 days	No	oxazine, adenine
H	Accumulation	Yes	7 days	No	oxidized C14-fatty acids
I	Consumption	Yes	7 days	Yes	creatine, dipeptides
J	Consumption	Yes	7-21 days	Yes	quinolines, cholines
K	Consumption	Yes	14 days	Yes	coumaryl acetate, hydrocinnamic acid

According to **Figure 5B** and **Table 1**, it can be seen that, in all cases, some of the metabolites that accumulate over time correspond to oxidized fatty acids. Among these, longer-chain fatty acids accumulated more rapidly than the shorter-chain ones. At the same time, small metabolites were rapidly consumed. Metabolites from group G were less consumed than those from group F, suggesting the latter to be more easily assimilated by the microorganisms in the digesters. Regarding the FW-specific metabolites (groups I-K), these were consumed at different paces. Dipeptides were

first exhausted, followed by molecules with choline groups or quinolines, and finally phenylpropanoids.

3.3.1. Metabolomics of oak and ash

Since the previous analysis did not reveal differences at the metabolomics level among ash and oak bioreactors, not even at higher PCs (results not shown), these were further sought for using the O-PLS-DA chemometric method (see Methods). The O-PLS-DA model composed of one orthogonal and one predictive component explained the 99.8% of the Y-variance (i.e., the wood type) with 27.3% of the X-variance (i.e., the metabolomic data). This strategy highlighted 55 metabolites associated with ash-containing substrate and 18 with oak-containing substrate. On the one hand, oak samples were found to be more enriched in furans, quinolines, and phenanthrenes. On the other hand, ash samples contained higher levels of sesquiterpenoids, alkaloids, coumaric acids, and plant hormones (e.g., abscisic acid), among others. In those samples, biologically active compounds such as isoflavones and coumaric acid derivatives are rapidly degraded while others such as benzaldehyde or sesquiterpenes are more recalcitrant (**FigS1** and **Table A.1**).

4. Discussion

The three types of studied data gave information about three different groups of molecules: 3D fluorescence spectroscopy revealed the signature of macromolecules, HPLC metabolomics revealed changes in the smaller molecules, and finally the biogas production data related to the final products of the degradation of the compounds detected in those two analytical techniques. Although both 3D fluorescence spectroscopy and HPLC metabolomics were used in this work because of their complementarity, there is an overlap between the metabolites measured with these two techniques, corresponding to the small metabolites with aromatic moieties (e.g., some amino acids and short peptides, polyphenols (Ku et al., 2019)).

384 In terms of the experimental setup, all anaerobic digesters were found to be very stable since a good
385 reproducibility of the results was observed for the three types of measurements, even one month after
386 the start of the experiment.

387 Among the three data sets, the biogas production data provides the most informative results regarding
388 the overall performance of the anaerobic digesters. This may be due to the fact that the biogas
389 production data reflects the cascade of all individual reactions occurring in the digesters while both
390 the HPLC-MS metabolomics data and the 3D fluorescence data captured the alterations of more
391 limited groups of molecules (small soluble compounds for HPLC-MS metabolomics and proteins and
392 humic/fulvic-like molecules for fluorescence spectroscopy).

393 Oak is more recalcitrant than ash since biogas production was lower for oak than for ash. This was
394 also observed in the co-digestion experiment as the second peak appeared later for FW-oak than for
395 FW-ash. This is in agreement with the fact that, in terms of molecular content, oak has more lignin,
396 flavonoid and phenolic content and less polysaccharides than ash (Madrera et al., 2010; Sillero et al.,
397 2019). Despite this aspect, the biogas production of oak was slightly increased (103%) by using the
398 co-digestion approach.

399 The cellulose substrate was more degradable than oak and ash woods, as seen by the two peaks of gas
400 production appearing before the 10^{th} day. Mixing cellulose with FW seems to have altered the order of
401 the compounds being degraded. We postulate that the degradation of cellulose alone is driven by a
402 microbial community specific for this substrate (i.e., cellulolytic) while in presence of FW, the
403 microbial community resembled more that involved in FW degradation. As a result of that,
404 compounds associated with the 2^{nd} peak in cellulose digestion were not fully degraded in FW-
405 cellulose as the microbial community was turning to degrade the more recalcitrant compounds from
406 the FW fraction. After these compounds were consumed, compounds from cellulose continued to be
407 degraded, producing the 4^{th} and final peak in FW-cellulose digestion. This phenomenon of continued
408 adaptation of the community to degrade the FW-cellulose mixture may have caused the levels of
409 biogas production to be around 89 % of the combined amount obtained by FW- and cellulose-mono-

digestions. Similarly, the daily biogas production of FW-ash AcoD as well as its overall lower biogas production if compared to the combined mono-digestion counterparts (93 %) suggests that both substrates are degraded by two different populations of microorganisms that are in competition with each other, that the microorganisms more adapted to degrade FW dominate in the FW-ash AcoD, and that at the end of the experiment the degradation of FW-ash was not completed.

The previous interpretations of the gas production can be confirmed by some observations made on the 3D fluorescence and the HPLCMS metabolomics data.

Regarding the 3D fluorescence data: 1) the least degradable substrates were oak, followed by ash, as hinted by the lower scores shown in IC1 and IC2 and by the higher scores in IC4 and IC5; 2) ash has more protein-like content than oak (as seen by the larger scores for IC1, IC2 and IC3), as well as more humic-like and lipofuscin-like content (depicted by IC5). The almost complete reduction of IC5 in ash AD might have been the cause that led to the production of the big peak in IC3. 3) the opposite trend observed in IC4 for cellulose AD and oak AD suggests that alpha cellulose (as in cellulose AD) can be rapidly degraded but not lignocellulose (as in oak), which led to different AD outcomes; 4) AcoDs gave very low scores in IC4 and IC5, suggesting that the co-digestion approach effectively aided in depleting the lignocellulosic material and other compounds of low degradability from the digester; 5) about the protein-like signature of the AcoDs, IC1 may represent the overall consummation of the protein content in the digesters, while IC2 and IC3 may together reflect the partial degradation of the protein-like content, occurring more prominently after the 14^{th} day, as observed decreases in IC2 seem to translate to equivalent increases in IC3 (Figure 2). As bigger increases occurred in IC3 for FW-ash and FW-oak, we can argue that this protein-like signature comes from compounds that were not accessible for the microbial community at the beginning of the digestion. The fact that these signatures are not associated with the initial degradation stage suggests that the corresponding compounds were not present in the liquid fraction at the beginning of the degradation, and that they were gradually released during the digestion.

Regarding the metabolomics data: 1) ash and oak are very poorly degraded as seen from the small time evolution of their scores; 2) cellulose degradation differs greatly from that of FW-cellulose since their PCA trajectories evolve in different sectors of the PCA plot; 3) the degradation profile of FW-cellulose, along with the other AcoD degradation profiles, resembles more the degradation profile of FW, indicating that adding this more degradable co-substrate promotes the growth of the microorganisms more adapted to degrade FW; 4) the addition of ash to FW AD produced a delay in the molecular events leading to an incomplete degradation of the substrate, as seen by the continued evolution of the PC2 scores for FW-ash AcoD even at the latest time-points.

In addition to information on the substrates' temporal degradabilities, the metabolomics data illustrated the chemical differences of the substrates as well as some of the underlying molecular degradation mechanisms occurring during AD: glycosylated compounds and other compounds from group B in **Figure 5** were specific to cellulose mono-digestions, detected from day 7. Compounds from group D were mainly specific to FW-containing bioreactors. Compounds from group A and C, relative to more ubiquitous compounds (e.g., phosphoric acid, oxidized fatty acids) were detected in all the tested conditions. Then, as seen in the analysis of section 3.3.1 regarding oak and ash woods, the former was richer in compounds of high aromaticity, in line with the observed recalcitrance (Marschner et al., 2008).

On a temporal scale, the observed metabolomics changes, either monotonic consumptions or accumulations, occurred from the start of the digestion and their duration depended on the metabolite levels in the substrate and on their degradability. For instance, compounds from groups F, G, I, J and K were consumed over time, reaching undetectable levels for groups I and J but not for the other 3 groups. Besides consumption, another metabolic alteration that is suggested by the metabolomics data is (lipid) oxidation.

Altogether, we can conclude that the investigation of the liquid fraction of the bioreactor allowed us to capture the metabolic signature of the hydrolysis step in AD, where extracellular enzymes (such as cellulases and proteases) produced by bacteria act on the substrates, converting water-insoluble

polymeric structures into smaller soluble metabolites, which microorganisms can subsequently take in and use as nutrients. Metabolites described by PC1 vary less over time than those related to PC2, denoting a more recalcitrant profile for the former metabolites. Regarding PC2, differences among the cellulose-rich substrates were small, as shown in the PCA score plot of **Figure 4**, due to their very similar chemical nature.

In this work we focused on the soluble faction, but alternative metabolomics approaches could have been employed for different purposes as well. For example, the metabolomics analysis of the solid fraction, which contains both the substrate being degraded and the microbial load, would have provided insights into how the metabolites, after being internalized, were directed towards biogas production through the AD stages of acidogenesis, acetogenesis, and methanogenesis (Puig-Castellví et al., 2022).

While we cannot directly establish a link between the metabolites detected in this study and biogas production because of this lack of information about the internalized metabolites, data suggests that metabolites used as substrate during early biogas production were from a more diverse mixture of compounds (specifically, metabolites from groups F, G, I, J, K in **Table 1**), and that later biogas production resulted from the degradation of less biodegradable compounds (metabolites from groups J and K in **Table 1**, as those from groups F, G, and I had already been exhausted). Still, for some substrates, the link between the metabolites and the biogas production could be drawn: The peak occurring between days 4 to 10 in cellulose AD might be associated to compounds described by IC4 from the analysis of the 3D fluorescence data (Figure 2) and to compounds from groups G, and I-K in the metabolomics data (Table 1). In both cases, compounds were consumed right before the peaks' formation. Then, for the two wood ADs, their widest peak of biogas production could be mainly associated to IC3 and IC5 from the analysis of the 3D fluorescence data (Figure 2) as these ICs are the most important for these substrates.

In this paper, we have demonstrated the applicability of two molecular characterization techniques to study the progress of anaerobic digestion from a biochemical perspective. These two techniques not

only have revealed the dynamics of the metabolite levels inside the reactors (relative to the macromolecules, with 3D fluorescence spectroscopy; and to the small metabolites, with metabolomics), but they also allowed us to identify the more recalcitrant metabolites. Similarly, metabolomics and 3D fluorescence can be explanatory of the metabolic changes induced by modifications in the operational conditions (e.g., reactor temperatures (Liu et al., 2015; Puig-Castellví et al., 2022), presence of inhibitory molecules such as ammonia (Chapleur et al., 2021; Su et al., 2019)). This knowledge can guide the selection of a more suitable microbial inoculum to these operational conditions, or more suitable conditions in general, resulting on a more efficient substrate degradation.

Compared to studies in the existing literature, we have proposed a data analysis strategy that allowed us to have a deeper understanding of the molecular changes. One the one hand, we used ICA instead of manually integrating the peaks from the 3D data (Chen et al., 2022) to identify alterations in the levels of compounds with overlapping fingerprints that might have otherwise gone unnoticed. Specifically, we separated the peaks related to the protein-like content (region III) into three components (IC1, IC2, and IC3). On the other hand, despite the chemical complexity of the substrates, we showed that the metabolomics could still be studied at the metabolite level to get insight into the biochemical changes, rather than using other less informative approaches such as the compounds' H/C and O/C ratios and plotting them in van Krevelen diagrams (Li et al., 2023).

3D fluorescence spectroscopy, due to its relatively low instrumentation cost and its high data output rate (in the of seconds), has the potential to be used in-line to routinely monitor AD (especially for monitoring degradations of substrates exhibiting strong fluorescent signatures, e.g., rich in proteins and/or with an abundance of humic acids) and to complement the information obtained with the traditional measurements (e.g., temperature, pH, COD). Although HPLC-MS metabolomics can characterize a larger number of compounds, the technique is more expensive and the time required to acquire and analyze the data is greater. Because of this, metabolomics should be applied more to investigate in-depth anomalous situations in digesters, that cannot be fully understood using the routine measurements. This type of application is currently covered with other omics approaches,

such as 16S DNA metabarcoding (Cardona et al., 2022). Having said this, HPLC-MS metabolomics gives a more direct insight into the degradation process than the omics approaches based on genetic information since, for the latter, the metabolic alterations are not measured but inferred from the modifications in the microbial community in terms of the DNA or RNA levels. Nevertheless, at present, these gene-based omics approaches are considered the gold standard in the field as their experimental protocols are already established. Conversely, for HPLC-MS metabolomics, their application in AD is very recent and further research is crucial to characterize the chain of degradation events linked to each substrate and molecular species, to better understand these processes from a biological and ecological perspective, and to use this knowledge for operational purposes, such as for finding monitorable metabolite biomarkers of process stability and (in)effective degradation.

5. Conclusions

3D fluorescence spectroscopy and HPLC-MS metabolomics are two complementary techniques that can be used to decipher substrate degradability. We found that cellulose was more degradable than ash and oak, oak being the most recalcitrant, possibly due to the presence of compounds with a high aromaticity (e.g., fulvic acids).

Regarding AcoD, the two approaches allowed us to obtain insight into how the substrate's chemical composition determines the outcome of the degradation. Adding FW to cellulose, ash wood, or oak wood resulted in several modifications in their molecular fingerprints, compared to their corresponding mono-digestion without the FW substrate. Specifically, the degradation profiles of the molecules in the AcoDs resembled those observed in FW AD (due to the higher abundance of glycerolipids, among other compounds) more than that in the digestion of the three other cellulose-rich substrates (containing more glycosylated compounds, among others).

Both 3D fluorescence spectroscopy and HPLC-MS metabolomics captured the early molecular changes in the bioreactors, which cannot be inferred from the biogas production data alone. These

changes could be grouped into 7 dynamics: 2 related to metabolite accumulation and 5 to metabolite exhaustion, and metabolites within each group presented similarities in their chemical structure. For this reason, to further investigate AcoD, more studies combining several high-throughput techniques should be undertaken in the future.

6. Appendices

Table A.1. Annotation of significant metabolomics features.

Fig S1. Heatmap of the selected features in the O-PLS-DA of ash vs oak samples.

Acknowledgements

We thank Christophe Cordella and Nathalie Locquet from AgroParisTech for providing us with access to the spectrofluorometer used in this study.

Declaration of competing interest

The authors declare that they have no known competing financial interests or personal relationships that could have appeared to influence the work reported in this paper.

References

Awhangbo, L., Bendoula, R., Roger, J.M., Béline, F., 2020. Detection of early imbalances in semi-continuous anaerobic co-digestion process based on instantaneous biogas production rate. Water Research 171, 115444. https://doi.org/10.1016/j.watres.2019.115444

Bhatia, S.K., Joo, H.-S., Yang, Y.-H., 2018. Biowaste-to-bioenergy using biological methods – A mini-review. Energy Conversion and Management 177, 640–660. https://doi.org/10.1016/j.enconman.2018.09.090

Borowski, S., Kubacki, P., 2015. Co-digestion of pig slaughterhouse waste with sewage sludge. Waste Management 40, 119–126. https://doi.org/10.1016/j.wasman.2015.03.021

562 Braguglia, C.M., Gallipoli, A., Gianico, A., Pagliaccia, P., 2018. Anaerobic bioconversion of food
563 waste into energy: A critical review. Bioresource Technology, Bioconversion of Food Wastes
564 248, 37–56. https://doi.org/10.1016/j.biortech.2017.06.145
565 Cardona, L., Mazéas, L., Chapleur, O., 2022. Deterministic processes drive the microbial assembly
566 during the recovery of an anaerobic digester after a severe ammonia shock. Bioresource
567 Technology 347, 126432. https://doi.org/10.1016/j.biortech.2021.126432
568 Chapleur, O., Poirier, S., Guenne, A., Lê Cao, K.-A., 2021. Time-course analysis of metabolomic and
569 microbial responses in anaerobic digesters exposed to ammonia. Chemosphere 283, 131309.
570 https://doi.org/10.1016/j.chemosphere.2021.131309
571 Chatterjee, B., Mazumder, D., 2019. Role of stage-separation in the ubiquitous development of
572 Anaerobic Digestion of Organic Fraction of Municipal Solid Waste: A critical review.
573 Renewable and Sustainable Energy Reviews 104, 439–469.
574 https://doi.org/10.1016/j.rser.2019.01.026
575 Chen, Y., Ping, Q., Li, D., Dai, X., Li, Y., 2022. Comprehensive insights into the impact of
576 pretreatment on anaerobic digestion of waste active sludge from perspectives of organic
577 matter composition, thermodynamics, and multi-omics. Water Research 226, 119240.
578 https://doi.org/10.1016/j.watres.2022.119240
579 Cruz, I.A., Andrade, L.R.S., Bharagava, R.N., Nadda, A.K., Bilal, M., Figueiredo, R.T., Ferreira,
580 L.F.R., 2021. An overview of process monitoring for anaerobic digestion. Biosystems
581 Engineering 207, 106–119. https://doi.org/10.1016/j.biosystemseng.2021.04.008
582 Dettmer, K., Aronov, P.A., Hammock, B.D., 2007. Mass spectrometry-based metabolomics. Mass
583 Spectrometry Reviews 26, 51–78. https://doi.org/10.1002/mas.20108
584 Du, Z., Zhao, P., Fu, Q., Wang, Q., Hu, A., Zhang, W., Wang, D., 2023. Biostimulants in dissolved
585 organic matters recovered from anaerobic digestion sludge with alkali-hydrothermal
586 treatment: Nontarget identification by ultrahigh-resolution mass spectrometry. Environment
587 International 173, 107813. https://doi.org/10.1016/j.envint.2023.107813
588 EEA, 2020. Bio-waste in Europe — turning challenges into opportunities. EEA Report No 4/2020,
589 European Environment Agency.
590 Iacovidou, E., Ohandja, D.-G., Voulvoulis, N., 2012. Food waste co-digestion with sewage sludge –
591 Realising its potential in the UK. Journal of Environmental Management 112, 267–274.
592 https://doi.org/10.1016/j.jenvman.2012.07.029
593 Jouan-Rimbaud Bouveresse, D., Moya-González, A., Ammari, F., Rutledge, D.N., 2012. Two novel
594 methods for the determination of the number of components in independent components
595 analysis models. Chemometrics and Intelligent Laboratory Systems 112, 24–32.
596 https://doi.org/10.1016/j.chemolab.2011.12.005
597 Kassouf, A., Jouan-Rimbaud Bouveresse, D., Rutledge, D.N., 2018. Determination of the optimal
598 number of components in independent components analysis. Talanta 179, 538–545.
599 https://doi.org/10.1016/j.talanta.2017.11.051
600 Ku, Y.G., Kim, H.C., Bae, J.H., Kang, B.S., Nemirovski, A., Barasch, D., Gorinstein, S., 2019.
601 Antioxidant capacities and polyphenols in autumn-growing cultivar of Chinese cabbage
602 (Brassica rapa L. ssp. pekinensis cv. Bulam Plus). Eur Food Res Technol 245, 1871–1879.
603 https://doi.org/10.1007/s00217-019-03294-0
604 Li, X., Huang, X., Zhao, C., Wang, X., Dong, B., Goonetilleke, A., Kim, K.-H., 2023. Characterizing
605 molecular transformation of dissolved organic matter during high-solid anaerobic digestion of
606 dewatered sludge using ESI FT-ICR MS. Chemosphere 320, 138101.
607 https://doi.org/10.1016/j.chemosphere.2023.138101
608 Liu, Y., Li, X., Kang, X., 2015. Effect of volume ratio on anaerobic co-digestion of thermal
609 hydrolysis of food waste with activated sludge. International Biodeterioration &
610 Biodegradation, CESE-2014 – Challenges in Environmental Science and Engineering Series
611 Conference 102, 154–158. https://doi.org/10.1016/j.ibiod.2015.02.015
612 Madrera, R.R., Valles, B.S., García, Y.D., del Valle Argüelles, P., Lobo, A.P., 2010. Alternative
613 woods for aging distillates-an insight into their phenolic profiles and antioxidant activities.
614 Food Sci Biotechnol 19, 1129–1134. https://doi.org/10.1007/s10068-010-0161-4

Madsen, M., Holm-Nielsen, J.B., Esbensen, K.H., 2011. Monitoring of anaerobic digestion processes: A review perspective. Renewable and Sustainable Energy Reviews 15, 3141–3155. https://doi.org/10.1016/j.rser.2011.04.026

Marschner, B., Brodowski, S., Dreves, A., Gleixner, G., Gude, A., Grootes, P.M., Hamer, U., Heim, A., Jandl, G., Ji, R., Kaiser, K., Kalbitz, K., Kramer, C., Leinweber, P., Rethemeyer, J., Schäffer, A., Schmidt, M.W.I., Schwark, L., Wiesenberg, G.L.B., 2008. How relevant is recalcitrance for the stabilization of organic matter in soils? Journal of Plant Nutrition and Soil Science 171, 91–110. https://doi.org/10.1002/jpln.200700049

Maynaud, G., Druilhe, C., Daumoin, M., Jimenez, J., Patureau, D., Torrijos, M., Pourcher, A.-M., Wéry, N., 2017. Characterisation of the biodegradability of post-treated digestates via the chemical accessibility and complexity of organic matter. Bioresource Technology 231, 65–74. https://doi.org/10.1016/j.biortech.2017.01.057

Moretti, P., Morais de Araujo, J., Borges de Castilhos, A., Buffière, P., Gourdon, R., Bayard, R., 2020. Characterization of municipal biowaste categories for their capacity to be converted into a feedstock aqueous slurry to produce methane by anaerobic digestion. Science of The Total Environment 716, 137084. https://doi.org/10.1016/j.scitotenv.2020.137084

Muller, M., Jimenez, J., Antonini, M., Dudal, Y., Latrille, E., Vedrenne, F., Steyer, J.-P., Patureau, D., 2014. Combining chemical sequential extractions with 3D fluorescence spectroscopy to characterize sludge organic matter. Waste Management 34, 2572–2580. https://doi.org/10.1016/j.wasman.2014.07.028

Peris-Díaz, M.D., Krężel, A., 2021. A guide to good practice in chemometric methods for vibrational spectroscopy, electrochemistry, and hyphenated mass spectrometry. TrAC Trends in Analytical Chemistry 135, 116157. https://doi.org/10.1016/j.trac.2020.116157

Puig-Castellví, F., Cardona, L., Jouan-Rimbaud Bouveresse, D., Cordella, C.B.Y., Mazéas, L., Rutledge, D.N., Chapleur, O., 2020. Assessment of substrate biodegradability improvement in anaerobic Co-digestion using a chemometrics-based metabolomic approach. Chemosphere 254, 126812. https://doi.org/10.1016/j.chemosphere.2020.126812

Puig-Castellví, F., Midoux, C., Guenne, A., Conteau, D., Franchi, O., Bureau, C., Madigou, C., Jouan-Rimbaud Bouveresse, D., Kroff, P., Mazéas, L., Rutledge, D.N., Gaval, G., Chapleur, O., 2022. Metataxonomics, metagenomics and metabolomics analysis of the influence of temperature modification in full-scale anaerobic digesters. Bioresource Technology 346, 126612. https://doi.org/10.1016/j.biortech.2021.126612

Rodriguez-Narvaez, O.M., Peralta-Hernandez, J.M., Goonetilleke, A., Bandala, E.R., 2017. Treatment technologies for emerging contaminants in water: A review. Chemical Engineering Journal 323, 361–380. https://doi.org/10.1016/j.cej.2017.04.106

Rorat, A., Courtois, P., Vandenbulcke, F., Lemiere, S., 2019. Sanitary and environmental aspects of sewage sludge management. Industrial and Municipal Sludge 155–180. https://doi.org/10.1016/B978-0-12-815907-1.00008-8

Rutledge, D.N., Jouan-Rimbaud Bouveresse, D., 2013. Independent Components Analysis with the JADE algorithm. TrAC Trends in Analytical Chemistry 50, 22–32. https://doi.org/10.1016/j.trac.2013.03.013

Sillero, L., Prado, R., Andrés, M.A., Labidi, J., 2019. Characterisation of bark of six species from mixed Atlantic forest. Industrial Crops and Products 137, 276–284. https://doi.org/10.1016/j.indcrop.2019.05.033

Slorach, P.C., Jeswani, H.K., Cuéllar-Franca, R., Azapagic, A., 2019. Environmental sustainability of anaerobic digestion of household food waste. Journal of Environmental Management 236, 798–814. https://doi.org/10.1016/j.jenvman.2019.02.001

Su, C., Zhao, L., Liao, L., Qin, J., Lu, Y., Deng, Q., Chen, M., Huang, Z., 2019. Application of biochar in a CIC reactor to relieve ammonia nitrogen stress and promote microbial community during food waste treatment. Journal of Cleaner Production 209, 353–362. https://doi.org/10.1016/j.jclepro.2018.10.269

Thévenot, E.A., Roux, A., Xu, Y., Ezan, E., Junot, C., 2015. Analysis of the Human Adult Urinary Metabolome Variations with Age, Body Mass Index, and Gender by Implementing a Comprehensive Workflow for Univariate and OPLS Statistical Analyses. J. Proteome Res. 14, 3322–3335. https://doi.org/10.1021/acs.jproteome.5b00354

Wishart, D.S., Guo, A., Oler, E., Wang, F., Anjum, A., Peters, H., Dizon, R., Sayeeda, Z., Tian, S., Lee, B.L., Berjanskii, M., Mah, R., Yamamoto, M., Jovel, J., Torres-Calzada, C., Hiebert-Giesbrecht, M., Lui, V.W., Varshavi, Dorna, Varshavi, Dorsa, Allen, D., Arndt, D., Khetarpal, N., Sivakumaran, A., Harford, K., Sanford, S., Yee, K., Cao, X., Budinski, Z., Liigand, J., Zhang, L., Zheng, J., Mandal, R., Karu, N., Dambrova, M., Schiöth, H.B., Greiner, R., Gautam, V., 2022. HMDB 5.0: the Human Metabolome Database for 2022. Nucleic Acids Research 50, D622–D631. https://doi.org/10.1093/nar/gkab1062

Zepp, R.G., Sheldon, W.M., Moran, M.A., 2004. Dissolved organic fluorophores in southeastern US coastal waters: correction method for eliminating Rayleigh and Raman scattering peaks in excitation–emission matrices. Marine Chemistry, CDOM in the Ocean: Characterization, Distribution and Transformation 89, 15–36. https://doi.org/10.1016/j.marchem.2004.02.006

Zhao, P., Du, Z., Fu, Q., Ai, J., Hu, A., Wang, D., Zhang, W., 2023. Molecular composition and chemodiversity of dissolved organic matter in wastewater sludge via Fourier transform ion cyclotron resonance mass spectrometry: Effects of extraction methods and electrospray ionization modes. Water Research 232, 119687. https://doi.org/10.1016/j.watres.2023.119687